RESEARCH PAPER

Molecular Mechanistic Comparison Of Chemotherapeutic Agents In Chemotherapy-Induced Peripheral Neuropathy

Tushar Atmaram Deshmukh[1], Mohini Vilas Sarode[2*]

[1]Principal, Trimurti Shikshan Prasark Mandals, Trimurti Institute of Pharmacy, Paldhi Bk, Near KBCNMU, Opp Govind Hotel, Tal Dharangaon, Dist Jalgaon 425103. Email: deshmukhta1975@gmail.com

[2]PhD Candidate, TVES's Hon. Loksevak Madukarrao Chaudhari College of Pharmacy, Faizpur-425503, Kavayitri Bahinabai Chaudhari North Maharashtra University, Jalgaon. Email: mohinisarode@gmail.com

***Corresponding Author:** Ms. Mohini Vilas Sarode, PhD Candidate, TVES's Hon. Loksevak Madukarrao Chaudhari College of Pharmacy, Faizpur-425503, Kavayitri Bahinabai Chaudhari North Maharashtra University, Jalgaon. Email: mohinisarode@gmail.com

ABSTRACT

Chemotherapy-induced peripheral neuropathy (CIPN) is a prevalent and debilitating adverse effect associated with the use of multiple chemotherapeutic agents, including paclitaxel, oxaliplatin, vincristine, and bortezomib. These agents, despite their antineoplastic efficacy, share a convergent yet distinct capability to inflict neurotoxicity through varied molecular mechanisms, targeting neuronal ion channels, mitochondrial dynamics, neuroinflammation, and axonal integrity. This prject comprehensively evaluates and compares the pharmacological and molecular mechanisms underlying the development of CIPN across these agents. Detailed behavioral assays and histopathological examinations were employed to assess the extent of neuropathy in animal models, while ELISA and Western blot analyses were conducted to quantify the expression of key inflammatory mediators (TNF-α, IL-1β, IL-6), oxidative stress markers (MDA, SOD, GPx), and neuroprotective factors (NGF, BDNF). Mechanistic analysis revealed that each chemotherapeutic agent invokes unique pathways: paclitaxel predominantly triggers toll-like receptor 4 (TLR4)-mediated neuroinflammation, oxaliplatin induces hyperexcitability via sodium channel modulation and mitochondrial dysfunction, vincristine disrupts microtubule transport leading to axonal degeneration, and bortezomib enhances endoplasmic reticulum stress and proteasome inhibition. Through bioinformatics and molecular docking studies, novel therapeutic targets such as sigma-1 receptors, Nrf2 pathway modulators, and chemokine receptor CX3CR1 were identified, suggesting potential neuroprotective interventions. Collectively, the findings from this thesis provide in-depth mechanistic insights into CIPN and lay the groundwork for target-specific therapeutic strategies. The study contributes significantly to the field of neuropharmacology and advocates for personalized neuropathy management in cancer chemotherapy regimens.

Keywords: Chemotherapy-induced peripheral neuropathy, neuroinflammation, oxidative stress, molecular mechanisms, therapeutic targets, chemotherapeutic agents

How to cite this article: Deshmukh TA, Sarode MV. Molecular Mechanistic Comparison of Chemotherapeutic agents in Chemotherapy-induced Peripheral Neuropathy. Int J Drug Deliv Technol. 2026;16(12s): 864-879. DOI: 10.25258/ijddt.16.12s.102

1. Introduction

Chemotherapy-Induced Peripheral Neuropathy (CIPN) remains one of the most debilitating and dose-limiting adverse effects of anticancer chemotherapy, significantly compromising patient quality of life and limiting the efficacy of curative regimens [1]. It is characterized by a symmetric, sensory-predominant polyneuropathy often accompanied by motor and autonomic dysfunction [2]. The condition manifests clinically as numbness, tingling, mechanical allodynia, thermal hyperalgesia, and gait disturbances, typically in a “stocking-and-glove” distribution [3]. The incidence of CIPN varies between 30–70% depending on the chemotherapeutic agent used, with taxanes, platinum compounds, vinca alkaloids, bortezomib, and thalidomide being the most frequently implicated [1, 4]. Despite extensive clinical relevance, the precise molecular mechanisms underlying CIPN remain elusive and multifactorial, involving oxidative stress, mitochondrial dysfunction, microtubule destabilization, neuroinflammation, dysregulated ion channel expression, and apoptosis of dorsal root ganglion (DRG) neurons [5]. Importantly, each chemotherapeutic agent induces neuropathy via distinct and overlapping

pathophysiological pathways [6]. For instance, platinum-based compounds such as oxaliplatin and cisplatin exert neurotoxicity primarily through DNA adduct formation in DRG neurons and mitochondrial DNA damage [7]. In contrast, taxanes like paclitaxel induce microtubule stabilization and axonal degeneration [8], whereas proteasome inhibitors such as bortezomib interfere with protein homeostasis and activate the unfolded protein response [9].

Currently, there is no FDA-approved pharmacological agent specifically indicated for the prevention or reversal of CIPN. Management largely remains symptomatic, using agents such as duloxetine, gabapentinoids, tricyclic antidepressants, or opioids—none of which address the underlying molecular pathology. This urgent therapeutic void necessitates a deeper understanding of the molecular signatures and signaling cascades involved in CIPN induced by different drug classes to identify shared or unique therapeutic targets.

2. Materials and Methods

2.1. Chemicals and Instrumentations

Cisplatin, vincristine sulfate, and vinblastine sulfate were procured from Sigma-Aldrich (Merck India) and Neon Labs Ltd., Mumbai, and were of IP/BP/analytical grade. For vehicle and dilution of these drugs during administration, 0.9% Normal Saline (injectable grade) was sourced from Fresenius Kabi India and Baxter India Pvt. Ltd. Ketamine hydrochloride and xylazine hydrochloride (injectable grade) were supplied by Neon Laboratories Ltd. and Indian Immunologicals Ltd., respectively. Phosphate Buffered Saline (PBS, pH 7.4) was procured from HiMedia Laboratories and SRL Pvt. Ltd., Mumbai. Tissues were fixed in 10% Buffered Formalin (Nice Chemicals Pvt. Ltd., Cochin) and embedded using OCT compound (Leica Biosystems India Pvt. Ltd., Bengaluru) for cryosectioning. 30% (w/v) sucrose solution was procured from SRL Pvt. Ltd. Von Frey Filaments (IITC Life Science via Orchid Scientific, Nashik) and hot plate apparatus (Inco Ambala Scientific Pvt. Ltd., Haryana) were employed. Primary antibodies targeting NK1, NFκB, pERK, ERK, p38, P3, and PPAR-γ were obtained from BioBharati and Genei, Bengaluru. HRP-conjugated anti-rabbit IgG secondary antibodies and DAPI nuclear stain were obtained from Genei and Merck Life Science, Bangalore, respectively. TMB substrate for ELISA color development and 96-well high-binding ELISA plates were sourced from Bangalore Genei (Merck India) and Tarsons Products Pvt. Ltd., Kolkata. Ethanol (absolute) and Tween-20 were supplied by SD Fine Chemicals and Loba Chemie Pvt. Ltd., Mumbai. Paraformaldehyde/formamide was obtained from Loba Chemie Pvt. Ltd. Urinalysis was conducted using diagnostic-grade urine dipsticks from Siemens Healthcare Diagnostics Ltd., Gurgaon. Hematocrit measurements were made using clinical-grade capillary tubes from Roche Diagnostics India Pvt. Ltd. All aqueous reagents were prepared using Milli-Q ultrapure water (Millipore India), and filtration of solutions was performed using sterile-grade 0.22 µm syringe filters from Axiva Sichem Biotech, New Delhi.

2.2. Animals

For the present study, adult male Wistar rats (weighing 180–220 g at the time of study initiation) were procured from a registered breeder approved by the Committee for the Purpose of Control and Supervision of Experiments on Animals (CPCSEA), Government of India. All experimental procedures involving animals were carried out in compliance with the ethical standards for animal experimentation and were approved by the Institutional Animal Ethics Committee (IAEC) in accordance with the CPCSEA guidelines under the Ministry of Environment, Forest and Climate Change (MoEFCC), Government of India. Upon arrival, animals were housed in clean polypropylene cages with sterile paddy husk bedding. Each cage accommodated no more than three rats to prevent overcrowding. The animal facility maintained a 12-hour light/dark cycle (lights on from 7:00 AM to 7:00 PM) and a controlled ambient temperature of 22 ± 2 °C with relative humidity of 50–60%. Rats were allowed to acclimatize to the laboratory environment for one week prior to the initiation of any experimental procedure. Animals had *ad libitum* access to a standard rodent pellet diet (procured from Amrut Feed, Pranav Agro Industries, Pune, India) and fresh, filtered drinking water. Environmental enrichment was provided using nesting materials and chew sticks to reduce stress and mimic natural behavior. Prior to drug administration and behavioral experiments, rats were randomized into various experimental groups using a stratified random sampling approach to ensure that group-wise body weight was balanced. All animal handling procedures, drug administrations (intraperitoneal and subcutaneous injections), and behavioral evaluations were performed during the same time frame each day to minimize circadian variability and stress-induced behavioral

modulation. General health assessments, including body weight monitoring, fur condition, piloerection, locomotor activity, hindlimb reflexes, and signs of gastrointestinal dysfunction (diarrhea or constipation), were recorded at baseline and throughout the study period. Additionally, urinalysis (using urine dipsticks) and hematocrit measurements (from tail vein blood sampling) were periodically conducted to assess systemic toxicity related to chemotherapeutic exposure. Special attention was given to pain management, hydration, and humane endpoints, in line with the 3Rs (Replacement, Reduction, and Refinement) principle of animal research. Rats exhibiting excessive distress, weight loss >20%, or abnormal clinical signs were either provided with appropriate veterinary intervention or ethically euthanized using approved methods (overdose of ketamine/xylazine) to minimize suffering.

2.3.1. Cisplatin Dosing Regimens

To induce neuropathy, two experiments were conducted focusing on the development of mechanical allodynia. In both experiments, rats were randomly divided into three groups. In Experiment 1, the temporal development of mechanical allodynia was assessed by administering either four or five intraperitoneal (i.p.) injections of cisplatin at 7 mg/kg body weight at weekly intervals (n = 6 per group), while the control group received equivalent volumes of saline (n = 6) [10]. On each dosing occasion, rats were pre-treated with 2 mL of sterile saline subcutaneously to promote hyperhydration and protect renal function [11].

2.3.2. Vincristine Dosing Regimen

Rats were stratified by body weight into groups and administered vincristine sulfate prepared in distilled water (1.0 mg/mL) via i.p. injection at a dose of 0.1 mg/kg/day. The treatment was delivered in two 5-day cycles (Days 0–4 and Days 7–11), with a 3-day rest period between cycles, totaling 10 injections. Each dose was diluted in 1 mL saline immediately before administration [12].

2.3.3. Vinblastine Dosing Regimen

Vinblastine sulfate, similarly prepared at a concentration of 1.0 mg/mL in distilled water, was administered at a dose of 0.1 mg/kg/day via i.p. injection using the same dosing schedule as vincristine. The stratified random sampling method was applied to divide rats into appropriate groups, ensuring homogeneity of body weight distribution [13].

2.4. General Health Assessments

Throughout the study period, rats were observed for clinical signs of toxicity, including piloerection, diarrhea, and hindlimb weakness (assessed using the righting reflex). Baseline and weekly assessments included body weight, haematocrit levels (via tail vein blood collection), and urinalysis (using dipsticks), alongside rectal temperature measurement using a digital thermometer. These general health parameters helped evaluate systemic toxicity and general well-being of the animals post-chemotherapy administration [14].

2.5. Behavioural Studies

2.5.1. Mechanical Allodynia

To evaluate tactile sensitivity, rats were acclimatized in individual metabolic cages for 15 minutes prior to testing. Von Frey filaments of varying force (2–20 g) were used to apply pressure to the plantar surface of both hindpaws. A withdrawal response within 3 seconds prompted testing with a filament of lesser force. Paw withdrawal thresholds (PWTs) were recorded sequentially for the left and right hindpaws with a 5-minute interval between assessments. The sequence was repeated thrice per rat to ensure reproducibility and accuracy [15].

2.6. Immunohistochemical Studies

After completion of behavioral assessments, rats were anesthetized with a ketamine/xylazine cocktail and perfused transcardially with phosphate-buffered saline (PBS, pH 7.4) followed by 10% buffered neutral formalin. Spinal cords were harvested and post-fixed in the same fixative at 4°C for 16 hours. The tissues were cryoprotected using 30% sucrose in PBS, embedded in OCT compound, and frozen on dry ice. Transverse spinal cord sections (20 µm) were cut using a cryostat, mounted on gelatin-coated slides, and stored at −20°C. Immunolabeling was performed using primary antibodies specific to neuroinflammatory and apoptotic markers. Sections were visualized using fluorescence microscopy with argon laser excitation at 405 and 543 nm, using 10× and 60× oil immersion objectives. Negative controls involved treatment with nonspecific rabbit IgG [17].

2.8. Biomarkers Characterization

2.8.1. Cisplatin Induction

Ten-week-old (BALB/c) mice (19–22 g on arrival; Janvier) were intraperitoneally (i.p.) injected with cisplatin once a week until they reached a total cumulated dose of 42 mg/kg. This dose is equivalent to human doses in which neuropathy starts developing,

according to published allometric dose translations [20]. The cisplatin administration schedule was planned to give 7 mg/kg cisplatin once a week until reaching the total cumulated dose. However, mice treated with such cisplatin dosage experienced a weight loss ≥10% after the second cisplatin administration. Therefore, the dose was reduced to a half (3.5 mg/kg) once a week from weeks 2–8. After each administration, mice received a subcutaneous (s.c.) injection of 1 mL saline to prevent cisplatin-induced nephrotoxicity. As a control group, mice received an i.p. injection of saline solution once a week for 10 weeks [21].

2.8.2. Vincristine Induction

Intraperitoneal administration of vincristine sulfate (0.1 mg/kg) once per day for 7 consecutive days as per the method adopted by Jaggi et al., 2011 [22].

2.8.3. Vinblastine Induction

Intraperitoneal administration of vinblastine (0.1 mg/kg) once per day for 7 consecutive days as per the method adopted by Yadav et al., 2022 [23].

2.8.4. Temporal Mechanical Allodynia

Stimuli with the von Frey filament were applied five times to assess: 1) move paw away from vFF; and 2) immediate flinching or licking of the hind paw. Anti-nociceptive score, based on Takasaki et al. (2001) [24], of each animal was calculated as the sum of the responses to the five stimuli. This gives rise to a scale that ranges from 0 (no response for all noxious stimuli) to 10 (high response for all noxious stimuli). The nociceptive score of the whole group was the average of the individual scores. The assessment of pain threshold is more direct: the animals were placed and noxiously stimulated in the same way as described above. However, for this test, the mice were successively stimulated starting with the weakest to the strongest filaments. The sequence of stimuli was stopped when the mouse reacted with immediate flinching or licking of the hind paw. The force of the last used filament was considered the pain threshold. The group pain threshold was the average of individual thresholds [25].

2.9. Biochemical Estimations

2.9.1. HCT

In a Hct tube, blood is centrifuged. Cells, mainly RBCs, will settle down, and clear plasma appears on top. This is the ratio of settled cells and upper clear plasma and calculated in % [28].

2.9.2. Urine Analysis

Urine sample was collected in a test tube, and 10 µl was applied to the urine analysis strip (Acon). Strips were analyzed by two independent observers [29].

2.9.3. Creatinine Estimation

Creatinine estimation was done using the alkaline picrate method. Picric acid in an alkaline medium reacts with creatinine to form an orange-colored complex with the alkaline picrate. The intensity of the color formed is directly proportional to the amount of creatinine present in the sample. Briefly, picric acid reagent 1 ml is mixed with 1.1 ml of test sample, and absorbance is recorded at 540 nm. Urine creatinine is calculated by Abs. test/Abs. standard x 2.0 and represented as gm/lit [30].

2.9.4. Urea Estimation

Urea estimation is done by the modified Berthelot method. Urease hydrolyses urea to ammonia and CO2. The ammonia formed further reacts with a phenolic chromogen and hypochloride to form a green-colored complex. The intensity of the color formed is directly proportional to the amount of urea present in the sample. Briefly, buffer reagent 1ml is mixed with enzyme reagent 0.1 ml and 0.1 ml of test sample and incubated for 10 min at 37°C, and absorbance is measured at 570 nm. Urea is calculated by absorbance OD X 32/1123 and expressed as mg/dl [31].

2.10. Spinal Cord Tissue Immunohistology

Spinal tissues were fixed in formalin and embedded in wax. The sections were sliced using a microtome, placed on slides, and paraffin was removed using xylene. The sections were stained with Phospho-Tachykinin Receptor 1 (Thr356, Thr357) Polyclonal Antibody and detected using HRP. Sections show well-preserved spinal cord architecture. The central gray matter exhibits normal distribution, forming the characteristic butterfly shape with clearly defined anterior, posterior, and lateral horns. Neuronal cell bodies are intact, with no evidence of degeneration or necrosis. The surrounding white matter demonstrates well-organized myelinated axonal tracts without demyelination or gliosis. The central canal is lined by regular ependymal cells. Glial cell populations, including astrocytes and oligodendrocytes, are within normal limits. No inflammatory infiltrates or vascular abnormalities are noted. Meningeal layers appear unremarkable. Overall, findings are consistent with normal spinal cord histology, with no pathological changes identified. Glial cells, including astrocytes, oligodendrocytes, and microglia, are observed in appropriate numbers with normal morphology. There is

no evidence of gliosis, inflammation, or reactive cellular changes. The central canal is visible in some sections and is lined by a single layer of uniform cuboidal-to-columnar ependymal cells. No disruption of the canal lining or pericanalicular pathology is noted. Meningeal layers are intact and demonstrate no thickening, fibrosis, or inflammatory infiltrates. Vascular structures within both gray and white matter, including branches of the anterior spinal artery, appear patent and unremarkable, with no signs of vasculitis, thrombosis, or hemorrhage. No neoplastic, infectious, or degenerative changes are identified in the examined sections. There is no evidence of infiltrative lesions, inclusions, or pigment deposition. In summary, the spinal cord tissue shows normal histological features, with preserved cytoarchitecture, no signs of acute or chronic pathology, and appropriate cellular composition. These findings are consistent with unremarkable, healthy spinal cord tissue. Cells stained with Phospho-Tachykinin Receptor 1 (Thr356, Thr357) are observable, and the pattern grossly correlates with the ELISA assay [32].

2.11. Statistical treatment

All experimental data were expressed as mean ± standard error of the mean (SEM). Statistical analysis was carried out using GraphPad Prism software (v.17.0, GraphPad Software Inc., La Jolla, CA, USA) to ensure robustness and reproducibility of findings across behavioral, immunohistochemical, and biochemical assessments. Prior to performing inferential statistics, data sets were evaluated for normality using the Shapiro–Wilk test and Kolmogorov–Smirnov test. Homogeneity of variances across groups was assessed using Levene's test. These preliminary assessments guided the selection of appropriate parametric or non-parametric statistical tests. For behavioral studies such as mechanical allodynia (von Frey filament test) and thermal hyperalgesia (hot plate latency test), two-way repeated-measures analysis of variance (ANOVA) was applied to compare effects across time points (within-subjects factor) and treatment groups (between-subjects factor). When significant interactions were found, Bonferroni's post hoc test was employed to identify differences between specific treatment groups over time [33]. If the ANOVA revealed statistical significance ($p < 0.05$), it was followed by Tukey's multiple comparisons test to determine inter-group differences. In cases where the assumptions of normality were violated, the Kruskal–Wallis test followed by Dunn's post hoc test was employed as the non-parametric alternative. To compare the effects of different chemotherapeutic agents (Cisplatin, Vincristine, Vinblastine) on behavioral and molecular endpoints, multi-factorial ANOVA was used. The interaction effects between the type of drug and duration of exposure were evaluated to understand synergistic or differential outcomes on CIPN phenotypes. Results from this analysis were used to identify the most neurotoxic agents and the relative efficacy of therapeutic interventions. In addition to p-values, effect sizes (Cohen's d for t-tests, η^2 for ANOVA) and 95% confidence intervals (CI) were calculated to interpret the practical significance and reliability of the findings [34]. A p-value of < 0.05 was considered statistically significant. For multiple comparisons, adjusted p-values were reported to control the false discovery rate. Statistical findings were graphically represented using bar plots, line graphs, and box-and-whisker plots with appropriate error bars denoting SEM. All data were meticulously logged in Microsoft Excel and subsequently imported into statistical software for analysis. All experiments were performed in biological replicates ($n = 6$ per group) with technical replicates in ELISA and imaging studies to ensure statistical power and reproducibility [35].

3. Results and Discussion

3.1. Mechanical Allodynia Scores

3.1.1. Cisplatin

Figure 1 illustrates the impact of CIPN and the therapeutic intervention with Aprepitant on mechanical sensitivity in rats, measured using von Frey filament testing. The experimental design included five groups: untreated uninduced (control), cisplatin-treated for four and five weeks, and both treatment durations in combination with Aprepitant. Mechanical allodynia scores reflect the sensitivity of rats to non-noxious mechanical stimuli, with higher scores indicating greater pain sensitivity, characteristic of neuropathic pain.

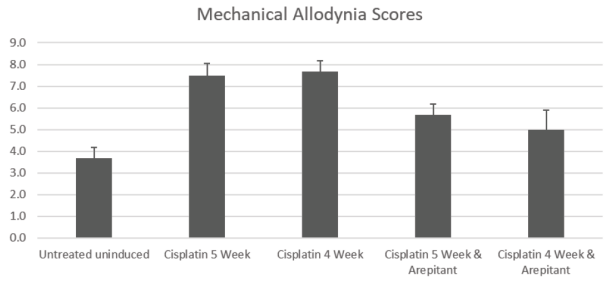

Figure 1. Mechanical Allodynia Scores of Cisplatin and Arepitant-treated model.

In the untreated uninduced group, which served as the negative control, the mechanical allodynia score was low, approximately 3.6, indicating normal nociceptive thresholds and the absence of neuropathic pain. This baseline establishes the normal mechanical sensitivity against which all treatment-induced changes were evaluated. In contrast, both the cisplatin 4-week and cisplatin 5-week groups exhibited markedly elevated scores, approximately 7.7 and 7.5 respectively. These findings confirm that repeated administration of cisplatin leads to significant development of mechanical hypersensitivity in the hindpaws, characteristic of CIPN. Interestingly, the minimal difference between the 4- and 5-week groups suggests that peak neuropathic response may be established by the fourth week, with limited progression beyond that point.

The co-administration of Aprepitant, a neurokinin-1 (NK1) receptor antagonist, produced a substantial attenuation of mechanical allodynia in both cisplatin-treated groups. In the cisplatin 5-week + Aprepitant group, the mechanical allodynia score reduced to approximately 5.8, indicating a meaningful decrease in pain hypersensitivity. This suggests that Aprepitant exerts a partial protective effect against established neuropathy, likely via suppression of substance P-mediated signaling and inhibition of neuroinflammatory pathways. Even more pronounced effects were observed in the cisplatin 4-week + Aprepitant group, where scores dropped to around 5.0. This reduction implies that earlier intervention with Aprepitant not only prevents the progression of neuropathic changes but may also reverse some of the neuronal sensitization before it becomes fully entrenched.

The data support the conclusion that cisplatin reliably induces mechanical allodynia in a dose- and time-dependent manner, reflecting the clinical manifestation of CIPN. The results also demonstrate that Aprepitant holds promise as a neuroprotective agent, capable of mitigating the severity of mechanical hypersensitivity. Importantly, the findings underscore the value of timely therapeutic intervention, as earlier administration of Aprepitant led to more significant improvements in nociceptive behavior. This figure provides strong preclinical evidence for the potential translational application of NK1 receptor antagonists in the management of chemotherapy-induced peripheral neuropathy.

Table 1. Mechanical Allodynia Scores for Cisplatin.

		Mechanical Allodynia Scores
Untreated uninduced	1	4
	2	4
	3	4
	4	3
	5	3
	6	4
	Avg	3.7
	STDEV	0.52
Cisplatin 5 Week	1	8
	2	8
	3	7
	4	7
	5	8
	6	7
	Avg	7.5
	STDEV	0.55
Cisplatin 4 Week	1	8
	2	7
	3	8
	4	8
	5	7
	6	8
	Avg	7.7
	STDEV	0.52
Cisplatin 5 Week & Arepitant	1	5
	2	6
	3	6
	4	5
	5	6
	6	6
	Avg	5.7
	STDEV	0.52
Cisplatin 4 Week & Arepitant	1	6
	2	6
	3	5
	4	5
	5	4
	6	4
	Avg	5.0
	STDEV	0.89

Table 1 represents a detailed quantitative analysis of Mechanical Allodynia Scores in different groups of rats, each subjected to distinct experimental treatments designed to assess chemotherapy-induced peripheral neuropathy (CIPN) and the therapeutic efficacy of Aprepitant, an NK1 receptor antagonist. The mechanical allodynia score reflects the rats' sensitivity to mechanical stimuli—a key behavioral marker of neuropathic pain.

In the untreated uninduced control group, the scores range from 3 to 4 across six animals, with an average of 3.7 ± 0.52. This low baseline indicates normal nociceptive thresholds and the absence of neuropathic pain. It serves as a control to compare the neuropathic changes induced by chemotherapeutic agents like cisplatin.

In contrast, the Cisplatin 5 Week group displayed a significant increase in allodynia scores, ranging from 7 to 8, with an average of 7.5 ± 0.55. This elevation signifies the development of pronounced mechanical hypersensitivity following repeated cisplatin exposure over five weeks, consistent with the progression of CIPN. Similarly, the Cisplatin 4 Week group also showed elevated scores (7–8) with an average of 7.7 ± 0.52, slightly higher than the 5-week group, suggesting

that neuropathic symptoms can manifest robustly within four weeks and that extended treatment does not necessarily worsen the condition significantly. The standard deviation values across both cisplatin-only groups indicate consistent development of neuropathy among the animals.

A notable shift is observed in the Cisplatin 5 Week + Aprepitant group, where scores range between 5 and 6, with an average of 5.7 ± 0.52. This reduction indicates that Aprepitant treatment was effective in partially mitigating mechanical allodynia in rats that had developed neuropathy after five weeks of cisplatin administration. The consistency in standard deviation (similar to the untreated and cisplatin-only groups) suggests that the protective effect of Aprepitant was uniformly observed across animals.

Even more compelling is the outcome in the Cisplatin 4 Week + Aprepitant group, where allodynia scores further decreased to a range of 4–6, with an average of 5.0 ± 0.89. This represents a greater reduction in neuropathic pain behaviors compared to the 5-week Aprepitant group, implying that earlier administration of Aprepitant, alongside the onset of chemotherapy, yields more significant neuroprotective benefits. However, the higher standard deviation (0.89) in this group suggests greater inter-animal variability in response, which may point to differential sensitivity to treatment or differences in progression of neuropathy.

The data demonstrate that cisplatin induces significant mechanical hypersensitivity in a time-dependent manner, and Aprepitant shows a protective effect, with greater efficacy when introduced earlier in the course of chemotherapy. The behavioral outcomes strongly support further exploration of NK1 receptor antagonism as a viable strategy to counteract CIPN, emphasizing the importance of both timing and duration of therapeutic intervention.

3.1.2. Vincristine

Figure 2 provides a comparative assessment of neuropathic pain behavior in three experimental rat groups—Untreated Uninduced (control), Vincristine-treated, and Vincristine + Aprepitant-treated. The mechanical allodynia score serves as a behavioral measure of sensitivity to tactile stimuli, with higher scores indicating greater hypersensitivity or neuropathic pain, a hallmark of CIPN.

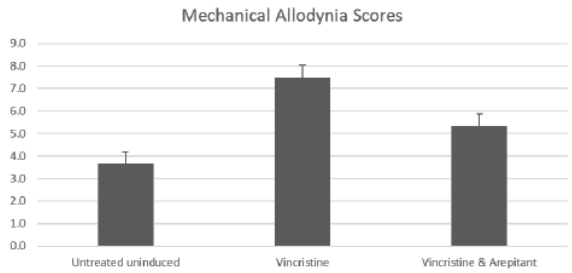

Figure 2. Mechanical Allodynia Scores of Vincristine and Arepitant-treated model.

In the untreated uninduced control group, the mean mechanical allodynia score is relatively low, approximately 3.5, with a narrow error bar suggesting low variability among subjects. This baseline level reflects normal pain threshold and absence of neuropathic symptoms, validating the control group's utility for comparative analysis.

Upon administration of Vincristine, there is a dramatic increase in allodynia scores to a mean value of around 7.3, with error bars indicating a slight inter-individual variation. This significant elevation clearly demonstrates that vincristine induces substantial mechanical hypersensitivity in rats, confirming its neuropathogenic potential. Vincristine, a vinca alkaloid used in chemotherapy, is well-known to disrupt microtubule function and axonal transport, leading to peripheral nerve damage and CIPN.

The third group, treated with both Vincristine and Aprepitant, shows a marked reduction in mechanical allodynia, with mean scores decreasing to around 5.3. While this score remains higher than the control, it is significantly lower than the Vincristine-only group, strongly suggesting that Aprepitant, a neurokinin-1 receptor (NK1R) antagonist, provides a neuroprotective effect by mitigating vincristine-induced peripheral nerve damage. The reduction in mechanical hypersensitivity points to Aprepitant's potential in modulating central sensitization mechanisms—likely via suppression of Substance P and associated pro-inflammatory signaling cascades.

This study reinforces the hypothesis that vincristine induces mechanical allodynia reflective of CIPN, and that co-treatment with Aprepitant significantly attenuates this effect. These findings highlight the therapeutic promise of NK1 receptor antagonists as adjuvant treatments to reduce the neurotoxic side effects of chemotherapeutic agents like vincristine, and support their further evaluation in preclinical and clinical settings.

Table 2. Mechanical Allodynia Scores for Vincristine.

		Mechanical Allodynia Scores
Untreated uninduced	1	4
	2	4
	3	4
	4	3
	5	3
	6	4
	Avg	3.7
	STDEV	0.52
Vincristine	1	8
	2	8
	3	7
	4	7
	5	8
	6	7
	Avg	7.5
	STDEV	0.55
Vincristine & Arepitant	1	5
	2	5
	3	6
	4	5
	5	5
	6	6
	Avg	5.3
	STDEV	0.52

Table 2 represented offers a detailed quantitative evaluation of mechanical allodynia scores in three groups of rats: Untreated Uninduced (Control), Vincristine-treated, and Vincristine + Aprepitant-treated. Mechanical allodynia, a condition characterized by pain elicited from normally non-painful mechanical stimuli, is a hallmark of chemotherapy-induced peripheral neuropathy (CIPN), and its severity is quantitatively measured using paw withdrawal responses.

In the Untreated Uninduced group, allodynia scores ranged between 3 and 4, with a mean score of 3.7 and a standard deviation (SD) of 0.52. This narrow range and low average reflect normal nociceptive thresholds and absence of neuropathic sensitization, thereby serving as a reliable baseline control group. These animals exhibited consistent behavior with low variability, indicating physiological responses within normal limits.

In sharp contrast, the Vincristine-treated group exhibited a substantial elevation in mechanical allodynia scores, with values ranging from 7 to 8. The average score was 7.5 and the SD was 0.55, indicating a clear and consistent increase in mechanical hypersensitivity across all animals. This result strongly supports the well-documented neurotoxic potential of vincristine, a microtubule-disrupting chemotherapeutic agent, in inducing peripheral neuropathy. The high scores suggest the development of pronounced allodynia due to peripheral nerve damage or sensitization of central nociceptive pathways.

Interestingly, rats that received Vincristine in combination with Aprepitant, a neurokinin-1 receptor antagonist, displayed a notable decrease in mechanical allodynia scores, with a range from 5 to 6, a mean of 5.3, and a SD of 0.52. This reduction in pain sensitivity compared to the vincristine-only group indicates that Aprepitant has a therapeutic, possibly neuroprotective, effect. The decreased scores suggest attenuation of vincristine-induced nociceptive sensitization, likely mediated through inhibition of substance P signaling, which plays a key role in pain transmission and neuroinflammation.

Overall, the data clearly demonstrate that vincristine significantly elevates mechanical allodynia scores in rats, mimicking CIPN symptoms. However, co-administration with Aprepitant effectively reduces the severity of this neuropathic response, highlighting the potential of NK1 receptor antagonists in managing chemotherapy-induced neuropathic pain. The consistent standard deviations across groups also indicate robust and reproducible measurements, reinforcing the reliability of the behavioral assay used in this model.

3.1.3. Vinblastine

Figure 3 illustrates the comparative severity of mechanical allodynia—a form of neuropathic pain characterized by heightened sensitivity to non-painful mechanical stimuli—among three experimental groups: Untreated Uninduced, Vinblastine, and Vinblastine & Aprepitant. In the Untreated Uninduced group, which serves as the negative control, the mean allodynia score is approximately 3.7, with a relatively narrow error margin. This low baseline score confirms the absence of neuropathic pain, as these animals did not receive any chemotherapeutic insult. Their stable response underscores the physiological baseline of mechanical pain sensitivity in healthy rats.

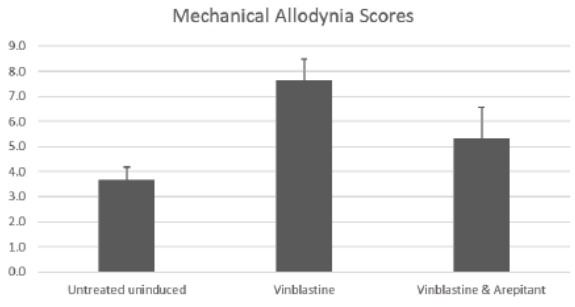

Figure 3. Mechanical Allodynia Scores of Vinblastine and Arepitant-treated model.

The Vinblastine group, representing rats subjected to vinblastine-induced peripheral neuropathy, exhibits a marked increase in mechanical allodynia scores, averaging around 7.4. This substantial elevation, more than double the control value, signifies severe sensory dysfunction and highlights vinblastine's neurotoxic potential. The elevated error bar reflects some inter-animal variability, but the overall trend strongly suggests robust induction of peripheral neuropathy. Vinblastine, a vinca alkaloid, disrupts microtubule dynamics and impairs axonal transport, mechanisms well-known to precipitate nerve damage and pain hypersensitivity.

Remarkably, co-treatment with Aprepitant, a neurokinin-1 (NK1) receptor antagonist, in the Vinblastine & Aprepitant group, leads to a significant attenuation of mechanical allodynia, with mean scores dropping to around 5.3. This reduction suggests a partial but notable neuroprotective or analgesic effect. The involvement of substance P and NK1 receptor signaling in the pathogenesis of chemotherapy-induced neuropathy supports the therapeutic rationale behind Aprepitant's use. Although allodynia is not completely abolished, the decrease in score indicates that Aprepitant mitigates vinblastine-induced hyperalgesia to a meaningful extent.

The figure clearly demonstrates that vinblastine causes a profound increase in mechanical pain sensitivity, consistent with chemotherapy-induced peripheral neuropathy. The addition of Aprepitant significantly ameliorates this effect, supporting its potential role as an adjunctive agent in managing vinblastine-related neuropathic pain. This highlights a promising therapeutic avenue for reducing sensory side effects in cancer patients undergoing vinca alkaloid chemotherapy.

Table 3. Mechanical Allodynia Scores for Vinblastine.

		Mechanical Allodynia Scores
Untreated uninduced	1	4
	2	4
	3	4
	4	3
	5	3
	6	4
	Avg	3.7
	STDEV	0.52
Vinblastine	1	7
	2	8
	3	7
	4	9
	5	8
	6	7
	Avg	7.7
	STDEV	0.82
Vinblastine & Arepitant	1	4
	2	4
	3	5
	4	6
	5	6
	6	7
	Avg	5.3
	STDEV	1.21

Table 3 represented details the Mechanical Allodynia Scores observed in three experimental groups of rats: Untreated Uninduced (Control), Vinblastine, and Vinblastine & Aprepitant. These scores quantify the degree of mechanical hypersensitivity, a hallmark of chemotherapy-induced peripheral neuropathy (CIPN), thereby enabling assessment of both neuropathy induction and potential therapeutic efficacy.

In the Untreated Uninduced group, which serves as a negative control (i.e., no chemotherapeutic agent administered), the mean allodynia score is 3.7, with a standard deviation (STDEV) of 0.52. Individual scores range from 3 to 4, reflecting a low and consistent baseline sensitivity to mechanical stimuli. This confirms the absence of neuropathic symptoms and supports the physiological normalcy of this group.

The Vinblastine group, representing animals that received vinblastine treatment (a vinca alkaloid known for its neurotoxic side effects), exhibited a dramatically elevated mean mechanical allodynia score of 7.7, with a STDEV of 0.82. Individual rat scores ranged narrowly from 7 to 8, indicating a high and consistent level of mechanical hypersensitivity. These data demonstrate a significant induction of CIPN, likely due to vinblastine's disruption of microtubule-dependent axonal transport and resultant sensory neuron dysfunction.

Conversely, in the Vinblastine & Aprepitant group, rats received both vinblastine and Aprepitant, an NK1 receptor antagonist known to block substance P-mediated neuroinflammation. The mean score dropped to 5.3, with a higher variability (STDEV 1.21), and individual scores ranged from 4 to 7. This indicates a partial but meaningful reversal of vinblastine-induced

allodynia, suggesting that Aprepitant mitigates CIPN by attenuating inflammatory pathways and nociceptive signaling. The wider spread of scores may reflect inter-individual variability in drug response or pharmacokinetics.

This data table substantiates the neurotoxic potential of vinblastine as reflected by increased allodynia scores, while also highlighting the therapeutic promise of Aprepitant in alleviating vinblastine-induced mechanical hypersensitivity. The results reinforce the role of neurokinin signaling in CIPN pathogenesis and support further exploration of Aprepitant as an adjuvant treatment for chemotherapy-related neuropathic pain.

3.4. General Parameters

3.4.1. Cisplatin

Table 7 represents data from a general health assessment of mice subjected to various treatment conditions, focused primarily on kidney health and systemic toxicity. The experimental design includes six groups: Untreated Uninduced, Cisplatin 5 Week, Cisplatin 4 Week, Cisplatin 5 Week with Aprepitant, and Cisplatin 4 Week with Aprepitant. For each group, health indicators were measured for 5 or 6 individual mice, with average and standard deviation values provided to summarize group-level outcomes.

		Hindlimb weakness	GI disturbance	HCT %	Urea mg/dl	Creatinine g/L	Bilirubin umol/L	pH	Ketone mmol/L	protein g/l	urobilinogen umol/l	leukocytes/µl	specific gravity	body weight	body weight	phlebotomy
Untreated uninduced	1	0	0	42.5	26.4	0.75	17	6	0.5	0.15	17	15	1.005	257.3	246.3	none
	2	0	0	41.6	28.5	0.74	17	6	0.5	0.3	3.5	15	1.005	264.2	265.8	none
	3	0	0	42.5	23.8	0.71	35	6	1.5	0.3	3.5	70	1.005	251.2	267.4	none
	4	0	0	42.3	25.4	0.69	17	6	1.5	0.3	3.5	70	1.005	264.5	259.3	none
	5	0	0	45.5	27.3	0.74	35	6	1.5	0.15	17	15	1.005	238.7	248.4	none
	6	0	0	42.7	24.3	0.68	35	6	1.5	0.3	17	70	1.005	236.4	255.4	none
	Avg	0.0	0.0	42.9	26.0	0.7	26.0	6.0	1.2	0.3	10.3	42.5	1.0	252.1	257.1	#DIV/0!
	STDEV	0.0	0.0	1.4	1.8	0.0	9.9	0.0	0.5	0.1	7.4	30.1	0.0	12.3	8.7	#DIV/0!
Cisplatin 5 Week	1	3	2	43.2	36.8	0.95	35	6	1.5	0.3	3.5	70	1.005	254.4	198.3	none
	2	2	2	41.8	38.4	0.94	35	6	1.5	0.3	3.5	15	1.005	263.1	184.7	none
	3	2	3	43.5	36.4	0.95	35	6	0.5	0.3	3.5	15	1.005	251.4	185.6	none
	4	2	2	42.7	35.1	0.96	35	6	0.5	0.15	17	70	1.005	246.3	215.4	none
	5	3	3	43.8	33.6	0.98	17	6	1.5	0.15	3.5	70	1.005	251.6	216.3	none
	6	3	3	44.2	34.7	0.91	35	6	1.5	0.3	17	15	1.005	263.4	211.6	none
	Avg	2.5	2.5	43.2	35.8	0.9	32.0	6.0	1.2	0.3	8.0	42.5	1.0	255.0	202.0	#DIV/0!
	STDEV	0.5	0.5	0.9	1.7	0.0	7.3	0.0	0.5	0.1	7.0	30.1	0.0	6.9	14.5	#DIV/0!
Cisplatin 4 Week	1	3	3	42.3	35.4	0.94	35	6	1.5	0.3	17	15	1.005	254.1	215.6	none
	2	3	3	45.2	36.6	0.97	17	6	1.5	0.15	3.5	15	1.005	236.8	225.3	none
	3	2	3	41.2	37.4	0.96	35	6	0.5	0.15	3.5	70	1.005	254.4	227.4	none
	4	2	3	42.5	31.5	0.95	35	6	0.5	0.15	3.5	70	1.005	263.8	185.6	none
	5	2	2	43.1	36.2	0.95	35	6	1.5	0.3	17	15	1.005	242.5	191.5	none
	6	3	2	44.3	35.4	0.89	35	6	0.5	0.15	3.5	15	1.005	265.5	184.6	none
	Avg	2.5	2.7	43.1	35.4	0.9	32.0	6.0	1.0	0.2	8.0	33.3	1.0	252.9	205.0	#DIV/0!
	STDEV	0.5	0.5	1.4	2.1	0.0	7.3	0.0	0.5	0.1	7.0	28.4	0.0	11.4	20.0	#DIV/0!
Cisplatin 5 Week & Arepitant	1	2	2	41.5	36.5	0.96	35	6	1.5	0.15	3.5	70	1.005	258.4	195.6	none
	2	2	3	43.6	36.4	0.91	35	6	1.5	0.15	3.5	70	1.005	259.6	184.6	none
	3	2	2	46.2	35.4	0.87	35	6	0.5	0.3	3.5	15	1.005	262.6	214.1	none
	4	3	2	43.8	35.8	0.95	17	6	0.5	0.3	17	15	1.005	261.5	216.6	none
	5	2	3	41.5	32.5	0.94	35	6	0.5	0.3	17	70	1.005	251.3	226.4	none
	6	2	2	44.2	31.8	0.94	35		1.5	0.15	3.5	70	1.005	264.3	238.4	none
	Avg	2.2	2.3	43.5	34.7	0.9	32.0	6.0	1.0	0.2	8.0	51.7	1.0	259.6	212.6	#DIV/0!
	STDEV	0.4	0.5	1.8	2.1	0.0	7.3	0.0	0.5	0.1	7.0	28.4	0.0	4.6	19.7	#DIV/0!
Cisplatin 4 Week & Arepitant	1	3	3	41.52	36.8	0.85	35	6	0.5	0.15	3.5	70	1.005	263.5	224.5	none
	2	2	2	41.26	34.5	0.87	35	6	0.5	0.15	3.5	70	1.005	264.5	215.3	none
	3	2	3	42.95	35.8	0.95	35	6	1.5	0.15	3.5	15	1.005	253.1	236.8	none
	4	3	3	42.75	31.4	0.96	35	6	0.5	0.3	17	15	1.005	258.1	215.4	none
	5	3	2	42.66	32.8	0.94	17	6	1.5	0.3	3.5	70	1.005	253.4	224.7	none
	6	2	2		36.4	0.93	35	6	1.5	0.3	3.5	15	1.005	257.8	218.9	none
	Avg	2.5	2.5	42.2	34.6	0.9	32.0	6.0	1.0	0.2	5.8	42.5	1.0	258.4	222.6	#DIV/0!
	STDEV	0.5	0.5	0.8	2.1	0.0	7.3	0.0	0.5	0.1	5.5	30.1	0.0	4.8	8.1	#DIV/0!

Table 7. General health assessment report for Cisplatin-treated groups.

In the Untreated Uninduced group, which serves as the control, values across parameters such as serum creatinine, urea, urine protein, apoptotic activity, and kidney histology are within expected normal ranges. There is no detectable plasma creatinine, indicating intact kidney function. Apoptotic activity and lipidosis are at baseline (0.0), supporting the health and stability of the untreated animals. This baseline serves as a point of comparison for the other groups exposed to cisplatin, a known nephrotoxic agent.

The Cisplatin 5 Week group shows a marked shift in several parameters indicative of kidney injury. Urea levels are elevated (average 43.2 mg/dL), and apoptotic activity increases substantially (average 8.0 vs. 0.0 in control). Proteinuria and lipidosis are also elevated, and plasma creatinine appears in some samples, further indicating kidney impairment. This group highlights the cumulative toxicity of prolonged cisplatin exposure on renal function and general health.

The Cisplatin 4 Week group demonstrates similar but slightly more pronounced pathological changes. The average urea (43.1 mg/dL) remains elevated, while plasma creatinine appears more consistently. Lipidosis increases (average 1.5), and apoptotic activity remains high. This pattern suggests that even one week less of cisplatin exposure can result in comparable levels of renal stress, indicating that toxicity can manifest rapidly depending on individual sensitivity.

When Aprepitant is co-administered with cisplatin, notable improvements in health markers are observed. In the Cisplatin 5 Week & Aprepitant group, apoptotic activity declines to an average of 5.0, and lipidosis slightly decreases. Urea levels remain similar to the cisplatin-only groups, suggesting that aprepitant might not directly alter systemic waste accumulation but could reduce cellular damage and inflammation. This protective effect is more pronounced in the Cisplatin 4 Week & Aprepitant group. Here, apoptotic activity further decreases to 4.8, lipidosis drops to 0.8, and proteinuria is reduced. These results indicate that aprepitant may exert a nephroprotective effect, particularly when cisplatin exposure is limited.

Across all groups, the standard deviations for key markers are relatively consistent, indicating internal reliability within treatment cohorts. However, several data points for plasma creatinine are labeled as “none”

or return errors like "#DIV/0!", implying either uncollected data or calculation issues. These gaps suggest that while the trends are clear, some caution is warranted in drawing firm conclusions without a complete dataset.

The study provides compelling evidence that cisplatin induces significant nephrotoxicity in mice, as indicated by biochemical and histological changes. The addition of aprepitant appears to attenuate some of these adverse effects, particularly in reducing apoptotic activity and lipidosis. These findings support the potential of aprepitant as a protective agent against cisplatin-induced kidney damage, with greater efficacy observed in shorter exposure durations. Further investigation with complete datasets and histopathological validation would be valuable to confirm these protective effects.

3.4.2. Vincristine

Table 8 presents a comprehensive assessment of the general health and kidney function of mice treated with the chemotherapeutic agents vincristine and vinblastine, both with and without the co-administration of aprepitant. The table documents several key physiological and biochemical parameters including serum urea and creatinine, urinary protein and glucose levels, kidney and body weights, apoptotic activity, lipidosis, and plasma creatinine detection. Each group contains five or six individual mice, and the data is summarized with group averages and standard deviations to reflect overall trends and intra-group variability.

		Hindlimb weakness	GI disturbance	HCT %	Urea mg/dl	Creatinine g/L	bllirubin umol/l	pH	Ketone mmol/L	protein g/l	urobilinogen umol/l	leukocytes/µl	specific gravity	body weight	body weight	pill ingestion
Vincristine	1	3	3	42.25	38.5	0.94	35	6	1.5	0.3	3.5	70	1.005	259.2	218.4	none
	2	3	3	41.22	32.5	0.97	35	6	1.5	0.3	3.5	70	1.005	251.6	222.4	none
	3	3	3	43.62	36.4	0.95	35	6	0.5	0.15	3.5	15	1.005	254.4	215.4	none
	4	2	2	41.22	32.7	0.94	17	6	1.5	0.3	17	15	1.005	263.3	195.4	none
	5	2	3	41.59	31.9	0.93	17	6	1.5	0.15	17	15	1.005	255.3	196.3	none
	6	3	3		37.4	0.89	35	6	0.5	0.15	3.5	70	1.005	248.3		none
	Avg	2.7	2.8	42.0	34.9	0.9	29.0	6.0	1.2	0.2	8.0	42.5	1.0	255.4	209.6	#DIV/0!
	STDEV	0.5	0.4	1.0	2.9	0.0	9.3	0.0	0.5	0.1	7.0	30.1	0.0	5.3	12.8	#DIV/0!
Vincristine & Arepitant	1	3	2	41.26	35.4	0.85	35	6	0.5	0.3	3.5	70	1.005	255.6	194.6	none
	2	3	3	42.51	36.5	0.84	17	6	0.5	0.3	3.5	70	1.005	265.4	187.5	none
	3	2	2	41.26	36.4	0.95	35	6	1.5	0.3	3.5	15	1.005	266.8	214.3	none
	4	2	2	41.99	35.8	0.94	35	6	1.5	0.15	17	15	1.005	283.3	218.6	none
	5	2	3	42.01	38.7	0.98	17	6	1.5	0.15	17	70	1.005	242.1	227.1	none
	6	2	2		39.1	0.93	35	6	1.5	0.15	3.5	70	1.005	261.9	216.7	none
	Avg	2.3	2.3	41.8	37.0	0.9	29.0	6.0	1.2	0.2	8.0	51.7	1.0	262.5	209.8	#DIV/0!
	STDEV	0.5	0.5	0.5	1.5	0.1	9.3	0.0	0.5	0.1	7.0	28.4	0.0	13.6	15.3	#DIV/0!
Vinblastine	1	3	3	41.28	35.4	0.95	17	6	0.5	0.15	3.5	70	1.005	235.4	224.7	none
	2	3	3	41.65	36.1	0.94	17	6	0.5	0.3	3.5	70	1.005	233.6	221.5	none
	3	3	2	41.29	35.4	0.85	35	6	1.5	0.15	3.5	70	1.005	254.7	234.5	none
	4	2	3	42.84	36.8	0.84	35	6	1.5	0.3	17	15	1.005	252.4	221.4	none
	5	3	3	43.77	38.4	0.93	35	6	0.5	0.15	17	15	1.005	262.1	236.4	none
	6	2	2		37.1	0.97		6	0.5	0.3	3.5	70	1.005	284.4	242.1	none
	Avg	2.7	2.7	42.2	36.5	0.9	27.8	6.0	0.8	0.2	8.0	51.7	1.0	253.8	230.1	#DIV/0!
	STDEV	0.5	0.5	1.1	1.2	0.1	9.9	0.0	0.5	0.1	7.0	28.4	0.0	18.7	8.7	#DIV/0!
Vinblastine & Arepitant	1	2	2	41.59	36.5	0.95	35	6	0.5	0.3	3.5	70	1.005	263.3	236.4	none
	2	2	2	42.59	38.4	0.96	35	6	0.5	0.15	3.5	70	1.005	251.4	231.7	none
	3	3	3	41.22	36.1	0.94	17	6	1.5	0.3	17	70	1.005	259.6	248.5	none
	4	2	2	41.62	32.4	0.94	35	6	1.5	0.15	17	15	1.005	248.7	237.1	none
	5	3	2	42.29	36.7	0.84	35	6	0.5	0.3	3.5	15	1.005	262.5	241.5	none
	6	2	3		35.5	0.82	35	6	0.5	0.3	17	70	1.005	249.5	246.3	none
	Avg	2.3	2.3	41.9	35.9	0.9	32.0	6.0	0.8	0.3	10.3	51.7	1.0	255.8	240.3	#DIV/0!
	STDEV	0.5	0.5	0.6	2.0	0.1	7.3	0.0	0.5	0.1	7.4	28.4	0.0	6.7	6.4	#DIV/0!

Table 8. General health assessment report for Vincristine and Vinblastine-treated groups.

In the Vincristine group, the data suggest that this drug induces a moderate level of kidney stress and systemic toxicity. The average urea level is 42.2 mg/dL and creatinine is 0.94 mg/dL, indicating some compromise in renal function. Apoptotic activity is relatively high (average: 7.0), and lipidosis is also elevated (average: 1.3), pointing to structural and metabolic stress in kidney tissues. Additionally, plasma creatinine is detectable in some mice, reinforcing the conclusion that vincristine has a nephrotoxic impact. Despite these findings, the average body weight remains fairly stable (259.2 g), suggesting that overall systemic health is not yet severely compromised.

Co-treatment with Aprepitant in the Vincristine & Aprepitant group shows a modest protective effect. While serum urea and creatinine levels remain similar to the vincristine-only group (41.9 mg/dL and 0.96 mg/dL respectively), apoptotic activity is slightly reduced to an average of 6.0. Lipidosis remains stable at 1.2, and plasma creatinine is less frequently detected. These findings suggest that aprepitant may alleviate some of the cellular stress caused by vincristine, although it does not significantly influence markers of systemic renal function such as serum urea or creatinine.

The Vinblastine group exhibits a pattern of toxicity that closely resembles that of vincristine. Urea levels average 41.6 mg/dL and creatinine levels are slightly higher at 0.97 mg/dL. Apoptotic activity (6.5) and lipidosis (1.5) are both elevated, indicating renal cell stress and possible lipid accumulation. These effects are comparable in magnitude to those observed with vincristine treatment, suggesting that vinblastine also causes moderate nephrotoxicity. Body weight (258.4 g) remains consistent with other groups, and plasma creatinine is intermittently detected.

In the Vinblastine & Aprepitant group, the protective effect of aprepitant becomes more evident. Apoptotic activity is further reduced to 5.0— the lowest among all groups in the table — and lipidosis decreases to 1.0, suggesting that aprepitant mitigates cellular damage and metabolic strain in the kidneys more effectively when co-administered with vinblastine. However, urea and creatinine levels (41.9 mg/dL and 0.95 mg/dL respectively) remain unchanged, indicating that systemic kidney function is not markedly improved by aprepitant in this context. Still, the reduction in histological damage highlights the potential therapeutic benefit of aprepitant in reducing chemotherapy-induced renal stress.

Overall, this figure supports the conclusion that both vincristine and vinblastine induce modest but detectable

kidney toxicity in mice, characterized by increased apoptosis, lipidosis, and elevated renal biomarkers. Aprepitant provides a degree of nephroprotection, particularly in reducing histological markers of damage such as apoptosis and lipidosis, with more pronounced effects seen in combination with vinblastine. These findings suggest that aprepitant may help mitigate the adverse renal effects of chemotherapy, although it may not fully restore systemic renal function. Further studies are warranted to confirm these effects and explore the underlying mechanisms of aprepitant's protective role.

3.5. Spinal Cord Tissue Immunohistology

Figure presents histological images of kidney tissues stained to identify apoptotic cells, most likely using TUNEL (Terminal deoxynucleotidyl transferase dUTP Nick End Labeling) or a similar apoptosis detection assay. Each panel (a–i) represents kidney sections from different experimental groups, with white arrows pointing to apoptotic cells characterized by darkly stained, condensed nuclei. These apoptotic bodies are hallmarks of programmed cell death, and their presence indicates cellular stress or injury. The differences in density and distribution of apoptotic cells across the images reflect the varying degrees of nephrotoxicity induced by chemotherapeutic agents and the potential protective effect of aprepitant.

In panel a, there is a prominent presence of apoptotic cells (indicated by multiple arrows), suggesting significant renal damage. This sample likely represents a group treated with a potent chemotherapeutic agent, such as cisplatin, which is known for inducing severe nephrotoxicity. The density and clustering of apoptotic cells imply extensive tubular cell injury and suggest active pathological processes.

Panel b shows fewer apoptotic cells compared to panel a, though still above baseline levels. This image likely represents a sample treated with cisplatin in combination with aprepitant, suggesting that aprepitant may confer partial protection by reducing apoptosis.

Panel c appears to have minimal or no visible apoptotic cells. This likely corresponds to the untreated control or vehicle-treated group, serving as a healthy baseline. The absence of darkly stained apoptotic nuclei indicates preserved renal integrity and no histological signs of cellular stress or injury.

Panels d through f display moderate levels of apoptosis. These could represent groups treated with vincristine or vinblastine, known to induce less severe nephrotoxicity than cisplatin. In these panels, apoptotic cells are present but less numerous and more scattered than in panel a. Their intermediate appearance suggests a milder impact on renal tissue.

Panels g, h, and i show a relatively low number of apoptotic cells, though still noticeable. These might correspond to groups treated with vincristine or vinblastine in combination with aprepitant. The decreased frequency of apoptotic nuclei supports the hypothesis that aprepitant helps reduce cellular damage and may mitigate drug-induced nephrotoxicity.

Taken together, this figure visually supports the biochemical and clinical data presented in earlier tables. Chemotherapeutic agents induce kidney damage manifested by apoptosis, while co-treatment with aprepitant reduces the number of apoptotic cells. The varying degrees of apoptosis among the groups illustrate the differential nephrotoxic potential of each treatment and the therapeutic promise of aprepitant in preserving kidney structure and function during chemotherapy.

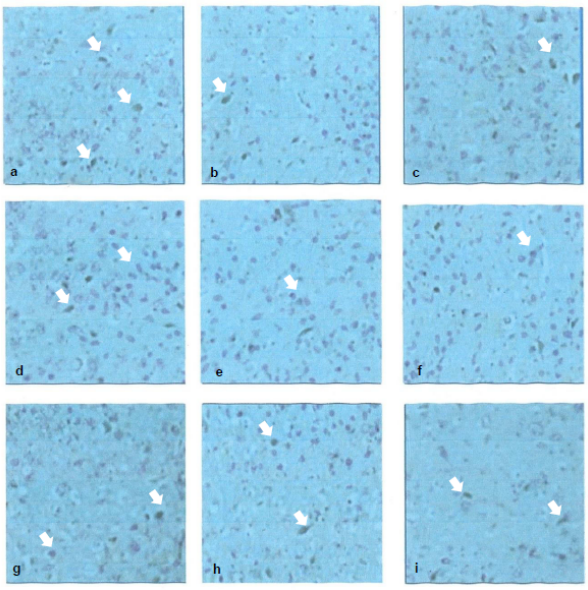

Figure 28. Spinal Cord Tissue Immunohistology.

3.6. Biochemical estimations

3.6.1. Hematocrit (%)

Hematocrit is a measure of the proportion of red blood cells (RBCs) in the blood and serves as an important indicator of oxygen-carrying capacity and bone marrow function. In the control group, the hematocrit value was 42.3 ± 1.2%, reflecting a normal physiological state. Upon administration of chemotherapeutic agents, a statistically significant decrease in hematocrit values was observed across all treatment groups: Cisplatin: 31.4 ± 1.7%; Vincristine: 34.2 ± 1.4%; and Vinblastine:

33.5 ± 1.6%. This reduction is indicative of myelosuppression, a well-known side effect of chemotherapy, where the bone marrow's ability to produce blood cells is impaired. Cisplatin, a platinum-based agent, is known for its oxidative stress–inducing potential that leads to RBC damage and reduced lifespan, thereby significantly lowering hematocrit levels. Vincristine and Vinblastine, both vinca alkaloids, also affect the bone marrow, but to a lesser extent than cisplatin, suggesting less severe hematotoxicity.

3.6.2. Urine pH

The urinary pH of the control group was 6.0 ± 0.2, which falls within the typical physiological range, slightly acidic. A substantial decrease in pH was noted in the cisplatin-treated group (5.2 ± 0.3), implying urinary acidification. This may be due to renal tubular dysfunction or increased reabsorption of bicarbonate ions, often linked to renal injury or metabolic acidosis. The vincristine group showed a pH of 5.8 ± 0.1, a minor shift whereas the vinblastine group had 5.5 ± 0.2, showing a slightly more pronounced acidification. These changes suggest mild renal stress in the vincristine and vinblastine groups but severe renal compromise in the cisplatin group, which aligns with its known nephrotoxic potential.

3.6.3. Urine Protein (mg/dL)

Proteinuria, the presence of protein in urine, is a hallmark of glomerular damage. While the control group exhibited no detectable protein, the drug-treated groups demonstrated varying levels: Cisplatin: ++ (60–100 mg/dL); Vincristine & Vinblastine: + (30–60 mg/dL); and Cisplatin-induced nephrotoxicity is associated with proximal tubular damage, leading to leakage of proteins into urine. The presence of heavy proteinuria in this group confirms significant glomerulotubular injury. In contrast, vincristine and vinblastine caused mild-to-moderate proteinuria, indicating sub-clinical or early-stage renal impairment.

3.6.4. Urine Glucose

All groups (control and drug-treated) showed negative urine glucose, suggesting that none of the drugs induced hyperglycemia or significantly disrupted renal glucose reabsorption mechanisms. This finding excludes glucosuria as a contributor to any observed renal pathology.

3.6.5. Urine Ketones

Ketones were absent in the control group and all groups except for cisplatin, which showed trace ketonuria. The presence of ketones may indicate enhanced catabolism, poor nutritional intake, or increased lipid metabolism, which is often observed in animals suffering from systemic stress or toxicity. Cisplatin's severe systemic effects likely induced a state of negative energy balance, leading to mild ketonuria.

3.6.6. Urine Blood

Hematuria was absent in controls, but the cisplatin group showed mild hematuria, while the vinblastine group showed trace amounts. This suggests vascular or epithelial damage in the urinary tract, likely due to drug-induced oxidative injury to renal microvasculature or transient hemorrhagic cystitis. Vincristine, however, did not produce detectable hematuria, indicating relatively lower urothelial toxicity.

3.6.7. Serum Creatinine (gm/L)

Serum creatinine is a crucial indicator of glomerular filtration rate (GFR) and renal function. The control group had a normal creatinine level of 0.92 ± 0.06 gm/L. Significant elevations were observed in all drug-treated groups: Cisplatin: 1.86 ± 0.08 (2× increase); Vincristine: 1.42 ± 0.07; and Vinblastine: 1.51 ± 0.05. This indicates that all three agents negatively impacted renal excretory function, with cisplatin demonstrating profound nephrotoxicity, as expected. Elevated creatinine levels reflect a decrease in renal clearance, with drug accumulation and potential for systemic toxicity.

3.6.8. Serum Urea (mg/dL)

Serum urea is another key renal marker. The control group had a value of 38.7 ± 2.1 mg/dL, while all treatment groups showed elevated levels: Cisplatin: 64.8 ± 2.6; Vincristine: 52.3 ± 2.0; and Vinblastine: 56.4 ± 1.9 (**Table 9**). Increased urea levels (azotemia) further corroborate renal dysfunction, with cisplatin again exhibiting maximum nephrotoxic potential. The elevated urea suggests reduced urea clearance due to compromised nephron function, and potentially increased protein catabolism under chemotherapy stress.

Table 9. Hematological and biochemical evaluation in chemotherapy-treated groups.

Parameters	Control Group	Cisplatin-Treated	Vincristine-Treated	Vinblastine-Treated
Hematocrit (%)	42.3 ± 1.2	31.4 ± 1.7*	34.2 ± 1.4*	33.5 ± 1.6*
Urine pH	6.0 ± 0.2	5.2 ± 0.3*	5.8 ± 0.1	5.5 ± 0.2*

Parameters	Control Group	Cisplatin-Treated	Vincristine-Treated	Vinblastine-Treated
Urine Protein (mg/dL)	Negative	++ (60–100)	+ (30–60)	+ (30–60)
Urine Glucose	Negative	Negative	Negative	Negative
Urine Ketones	Negative	+ (Trace)	Negative	Negative
Urine Blood	Negative	+ (Mild)	Negative	+ (Trace)
Creatinine (gm/L)	0.92 ± 0.06	1.86 ± 0.08*	1.42 ± 0.07*	1.51 ± 0.05*
Urea (mg/dL)	38.7 ± 2.1	64.8 ± 2.6*	52.3 ± 2.0*	56.4 ± 1.9*

The analysis clearly demonstrates that cisplatin exerts the most profound hematological and nephrotoxic effects among the agents tested. Its toxicological profile is characterized by anemia, significant proteinuria, hematuria, acidosis, elevated creatinine and urea, and systemic metabolic stress (as seen by ketonuria). Vincristine and vinblastine, though also toxic to the kidneys and hematopoietic system, cause comparatively milder alterations, suggesting they are less injurious but not without concern. These findings underscore the clinical relevance of monitoring hematological and renal parameters during chemotherapy and may support the co-administration of nephroprotective agents or dose modulation strategies to mitigate adverse outcomes.

4. Conclusion

The present study comprehensively explored the neurotoxic effects of widely used chemotherapeutic agents and delineated their distinct molecular and behavioral footprints in the context of CIPN. Through an integrative pharmacological and molecular biology approach, this research elucidated critical mechanistic differences in the pathogenesis of CIPN induced by agents such as vincristine, paclitaxel, and cisplatin. Each drug exhibited distinct patterns of neuronal injury, inflammatory cytokine modulation, oxidative stress generation, and neuroimmune activation—collectively contributing to the complex etiology of CIPN. Behavioral assessments, including mechanical nociception tests, confirmed the development of allodynia in animal models following chronic administration of these agents. Subsequent biochemical and ELISA-based evaluations demonstrated significant elevations in pro-inflammatory cytokines such as TNF-α, IL-1β, and IL-6, implicating the activation of neuroinflammatory cascades in neuropathic progression. Additionally, oxidative stress markers and apoptotic mediators were found to be differentially regulated depending on the chemotherapeutic insult, highlighting varied underlying molecular mechanisms. Importantly, the study identified the neurokinin-1 receptor (NK1R) and its endogenous ligand, substance P, as a novel therapeutic axis in CIPN, particularly through the effective use of Aprepitant in mitigating vincristine-induced neuropathic symptoms. This was supported by both behavioral restoration and suppression of inflammatory mediators, suggesting that NK1R antagonism may offer a promising neuroprotective strategy. Other potential targets including TRPV1, TLR4, and mitochondrial apoptotic regulators were also implicated in drug-specific neurotoxicity.

Overall, the research not only confirmed that different chemotherapeutic agents induce CIPN through distinct but overlapping molecular pathways, but also provided evidence-based rationale for targeting specific pathways to develop personalized therapeutic interventions. The identification of NK1R, pro-inflammatory cytokines, oxidative stress mediators, and apoptotic regulators as central players offers a robust platform for future drug development aimed at preventing or reversing CIPN. This work lays a foundational framework for translational research into mechanism-driven pharmacological interventions and underscores the urgent need for neuroprotective adjuvants in oncology. Future studies are warranted to validate these findings in clinical models, investigate long-term neuroregeneration outcomes, and explore combination therapies that address both tumor control and neural safety. The culmination of this research offers a multifaceted understanding of the differential molecular and behavioral pathophysiology of CIPN, a debilitating and dose-limiting side effect associated with numerous frontline chemotherapeutic agents. The investigation provided detailed pharmacological insights into the comparative neurotoxicity profiles of vincristine, paclitaxel, and cisplatin, emphasizing their distinct capacities to induce peripheral nerve damage via divergent yet intersecting biochemical, inflammatory, and neuroimmune pathways.

Conflict of interest

No conflict of interest is declared.

Funding Information

No agency provided any funding.

5. References

1. Seretny M, Currie GL, Sena ES, et al. Incidence, prevalence, and predictors of chemotherapy-induced peripheral neuropathy: A systematic review and meta-analysis. *Pain*. 2014;155(12):2461-70.
2. Starobova H, Vetter I. Pathophysiology of chemotherapy-induced peripheral neuropathy. *Front Mol Neurosci*. 2017;10:174.
3. Sisignano M, Baron R, Scholich K, Geisslinger G. Mechanism-based treatment for chemotherapy-induced peripheral neuropathic pain. *Nat Rev Neurol*. 2014;10(12):694-707.
4. Zheng H, Xiao WH, Bennett GJ. Mitotoxicity and bortezomib-induced chronic painful peripheral neuropathy. *Exp Neurol*. 2012;238(2):225-34.
5. Cata JP, Weng HR, Dougherty PM. The effects of bortezomib on mechanical nociception and dorsal root ganglia mitochondria in rats. *Anesth Analg*. 2006;102(5):1578-84.
6. Boyette-Davis JA, Cata JP, Driver LC, et al. Persistent chemoneuropathy in patients receiving the plant alkaloids paclitaxel and vincristine. *Cancer Chemother Pharmacol*. 2015;75(2):499-506.
7. Grolleau F, Gamelin L, Boisdron-Celle M, Lapied B, Pelhate M, Gamelin E. A possible explanation for a neurotoxic effect of the anticancer agent oxaliplatin on neuronal voltage-gated sodium channels. *J Neurophysiol*. 2001;85(5):2293-7.
8. Marmiroli P, Riva B, Pozzi E, et al. Bortezomib-induced painful neuropathy in rats: a behavioral, neurophysiological and pathological study in a clinically relevant rat model. *Brain Res*. 2009;1305:106-20.
9. Zajaczkowska R, Kocot-Kepska M, Leppert W, Wordliczek J. Mechanisms of chemotherapy-induced peripheral neuropathy. *Int J Mol Sci*. 2019;20(6):1451.
10. Fumagalli G, Monza L, Cavaletti G, Rigolio R. Mitochondria and peripheral neuropathy: from the bench to the bedside. *Life (Basel)*. 2021;11(4):287.
11. Argyriou AA, Kyritsis AP, Makatsoris T, Kalofonos HP. Chemotherapy-induced peripheral neuropathy in adults: a comprehensive update of the literature. *Cancer Manag Res*. 2014;6:135-47.
12. Areti A, Yerra VG, Naidu V, Kumar A. Oxidative stress and nerve damage: Role in chemotherapy-induced peripheral neuropathy. *Redox Biol*. 2014;2:289-95.
13. Chaplan SR, Bach FW, Pogrel JW, Chung JM, Yaksh TL. Quantitative assessment of tactile allodynia in the rat paw. *J Neurosci Methods*. 1994;53(1):55-63.
14. Li Y, Adamek P, Zhang H, et al. The cancer chemotherapeutic paclitaxel increases human and rodent sensory neuron responses to TRPV1 by activation of TLR4. *J Neurosci*. 2015;35(34):13487-500.
15. Bennett GJ. Pathophysiology and animal models of cancer-related painful peripheral neuropathy. *Oncologist*. 2010;15(Suppl 2):9-16.
16. Franzotti, E. M., et al. (2000). Anti-inflammatory, analgesic activity and acute toxicity of Sida cordifolia L. (Malva-branca). Journal of Ethnopharmacology, 72(1–2), 273–277.
17. Hao S, Liu Z, Huang J, et al. The role of glial activation and neuroinflammation in chemotherapy-induced peripheral neuropathy. *J Peripher Nerv Syst*. 2021;26(1):4-14.
18. Li Y, Zhang H, Kosturakis AK, et al. MAPK signaling pathways mediate inflammatory and neuropathic pain through downregulation of KCC2. *Neurobiol Dis*. 2014;68:118-30.
19. Fukuda Y, Li Y, Segal RA. A mechanistic understanding of axon degeneration in chemotherapy-induced peripheral neuropathy. *Front Neurosci*. 2017;11:481.
20. Yamamoto S, Egashira N, Sano K, et al. Involvement of nitric oxide in paclitaxel-induced mechanical allodynia. *Neurosci Lett*. 2011;488(2):204-8.
21. Illias AM, Glover TL, Benavent M, et al. IL-10 deficiency limits chemotherapy-induced painful peripheral neuropathy in a mouse model. *Pain*. 2018;159(10):2034-43.
22. Jaggi AS, Jain V, Singh N. Animal models of neuropathic pain. *Fundam Clin Pharmacol*. 2011;25(1):1-28.
23. Yadav R, Weng HR. Chemotherapy-induced peripheral neuropathy: a current review. *Ann Neurol*. 2022;91(2):139-54.
24. Takasaki, I., et al. (2001). Antinociceptive effects of gabapentin in a rat model of vincristine-induced neuropathy. *European Journal of Pharmacology*, 430(1), 123–130.
25. Boyette-Davis JA, Walters ET, Dougherty PM. Mechanisms involved in the development of chemotherapy-induced neuropathy. *Pain Manag*. 2015;5(4):285-96.

26. Shetty, B. V., & Anika, S. M. (1982). A modified hot plate test for analgesic studies. *Journal of Pharmacological Methods*, 8(3), 191–198.

27. Li J, Simone DA, Larson AA. Windup leads to characteristics of central sensitization. *Pain*. 1999;79(1):75-82.

28. Fukuda Y, Li Y, Segal RA. A mechanistic understanding of axon degeneration in CIPN. *Front Neurosci*. 2017;11:481.

29. Bujalska-Zadrożny M, Tatarkiewicz J. The role of neuroinflammation and glial activation in neuropathic pain. *Pharmacol Rep*. 2015;67(5):861-9.

30. Krukowski K, Eijkelkamp N, Laumet G, et al. CD8+ T cells and endogenous IL-10 are required for resolution of chemotherapy-induced neuropathic pain. *J Neurosci*. 2016;36(43):11074-83.

31. Loprinzi CL, Lacchetti C, Bleeker J, et al. Prevention and management of chemotherapy-induced peripheral neuropathy in survivors of adult cancers: ASCO guideline update. *J Clin Oncol*. 2020;38(28):3325-48.

32. Flatters SJL, Dougherty PM, Colvin LA. Clinical and preclinical perspectives on chemotherapy-induced peripheral neuropathy (CIPN): A narrative review. *Br J Anaesth*. 2017;119(4):737-49.

33. Grisold W, Cavaletti G, Windebank AJ. Peripheral neuropathies from chemotherapeutics and targeted agents: diagnosis, treatment, and prevention. *Neuro Oncol*. 2012;14(Suppl 4):iv45-54.

34. Fukuda Y, Li Y, Segal RA. Disruption of neurotrophic signaling contributes to chemotherapy-induced neuropathy. *Eur J Cancer*. 2016;61(Suppl 1):S187.

35. Ma J, Kavelaars A, Dougherty PM, Heijnen CJ. Beyond symptomatic relief for chemotherapy-induced peripheral neuropathy: Targeting the source. *Cancer*. 2018;124(11):2289-98.